JOURNAL OF MAGNETIC RESONANCE, Series B 104, 193–198 (1994)

Improvements in HSMQC-Type Double- and Triple-Resonance NMR Experiments by Using Full-Sweep (Semi-)Constant-Time Shift Labeling

STEVEN R. VAN DOREN AND ERIK R. P. ZUIDERWEG*

Biophysics Research Division, The University of Michigan, 930 North University Avenue, Ann Arbor, Michigan 48109-1055

Received February 14, 1994

In efforts to enhance the sensitivity or resolution of heteronuclear correlation experiments, progress has been made in overlapping chemical-shift labeling periods with scalar-evolution periods. Grzesiek and Bax (*1*) as well as Logan *et al.* (*2*) have introduced such overlapping periods to shorten the duration of transverse relaxation in INEPT transfer steps by $(2J)^{-1}$, dubbed semiconstant-time or shared incrementation times. In other progress in overlapping evolution periods, Madsen and Sørensen (*3*) demonstrated a method of doubling the resolution in constant-time dimensions of "out-and-back" triple-resonance experiments. The method amounts to letting the "transfer" from an I spin, measured in the constant-time period, to an S spin be of the HMQC type and then using the chemical-shift evolution during both the defocusing and refocusing periods. We refer to this method as full-sweep constant time (FCT). Vuister and Bax (*4*) demonstrated a variation of this method which requires an additional π pulse on I as well as one on S, which we refer to as double constant time. A synthesis of semiconstant time and double constant time was recently proposed but not demonstrated (*5*).

In many experiments edited with a heterospin S, HSQC-type transfers are preferred over HMQC transfers since HSQC gives better lineshapes for the S spin because it is not affected by the passive couplings to the I spin or because single-quantum S magnetization relaxes more favorably. However, the methods for doubling of resolution in the constant-time dimension by utilizing both the dephasing and the rephasing periods cannot be used with the HSQC-type experiments. The HSMQC represents a compromise in that it constructs a linear combination of multiple- and single-quantum coherence with a lineshape improved over that of the HMQC (*6*). Furthermore, HSMQC uses fewer RF pulses than HSQC. We demonstrate that the methods of doubling resolution can be used with HSMQC versions of "out-and-back"-style triple-resonance experiments. Further, we demonstrate full-sweep semiconstant-time periods in labeling ^{1}H chemical shift in H(S)MQC-NOESY resulting in a line narrowing from a total time savings of nearly $1/J$.

A brief product-operator description for an HSMQC block with a full-sweep, semiconstant-time period (FSCT) refers to Fig. 1. As of point A, assuming that $t_1^a - t_1^b + t_1^c = (2J_{IS})^{-1}$, I_y has dephased with respect to S with these terms present:

$$-2I_xS_z\cos\,\Omega_I(t_1^a + t_1^b - t_1^c) + 2I_yS_z\sin\,\Omega_I(t_1^a + t_1^b - t_1^c). \quad [1]$$

At point B, the relevant multiple- and single-quantum terms are, respectively,

$$[2I_xS_y\cos\,\Omega_I(t_1^a + t_1^b - t_1^c) + 2I_zS_y\sin\,\Omega_I(t_1^a + t_1^b - t_1^c)]\cos\,\Omega_S t_2. \quad [2]$$

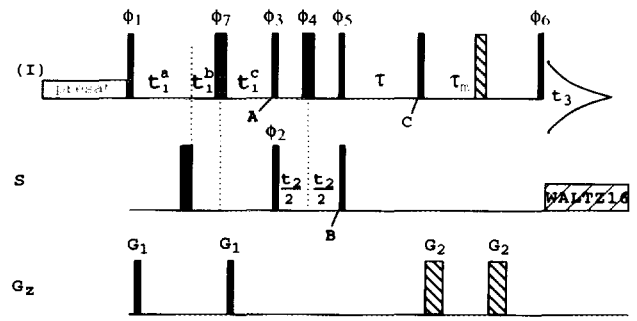

FIG. 1. Pulse sequence of the HSMQC-NOESY using full-sweep semiconstant-time measurement of ^{1}H chemical shift. The phase cycle is $\phi_1 = x, x, -x, -x; \phi_2 = x, -x; \phi_3 = 4(x), 4(y); \phi_4 = 4(x), 4(y); \phi_5 = 4(-x), 4(-y); \phi_6 = 8(x), [8(y)]; \phi_7 = x$; and receiver = $x, -x, -x, x, -x, x, x, -x, [y, -y, -y, y, -y, y, y, -y]$, where the optional step for quadrature image suppression is bracketed. States quadrature (*12*) is applied to ϕ_1 and States–TPPI (*13*) is applied to ϕ_2. Optional gradient pulses and optional composite π pulse during τ_m used for the sample in ^1H_2O are hatched. Length and magnitude of z gradient pulses were $G_1 = 100$ μs, 8 G/cm; and $G_2 = 3$ ms, 12 G/cm. In the absence of pulsed field gradients, $\phi_6 = x$; $\phi_7 = 8(x), 8(y), 8(-x), 8(-y)$; and receiver = $x, -x, -x, x, 2[-x, x, x, -x], 2[x, -x, -x, x], 2[-x, x, x, -x], x, -x, -x, x$.

* To whom correspondence should be addressed.

1064-1866/94 $6.00

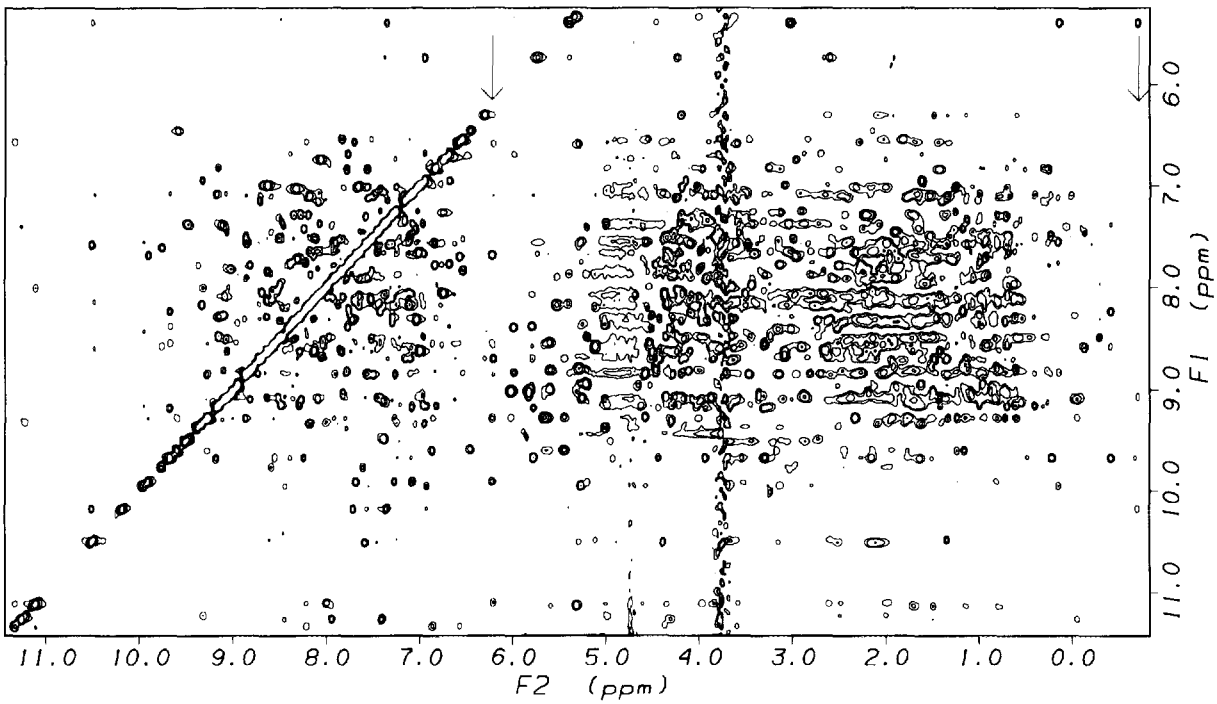

FIG. 2. ^{15}N HSMQC-NOESY spectrum acquired in full-sweep semiconstant-time (FSCT) fashion in 29.5 hours each on 1.8 m*M E. coli* flavodoxin, 5% D_2O, 20 m*M* protonated Tris·HCl, pH 8.0, 25°C. The spectrum was acquired on a Bruker AMX-500 equipped with a Bruker GRASP unit and triple-resonance probe. The NOE mixing time, τ_m, was 100 ms. Presaturation of the water with an RF field strength of 6 Hz was performed. The optional 16-step phase cycle, composite π pulse, and gradient pulses during τ_m described in the legend to Fig. 1 were used. During t_1, 192 complex points were collected using a spectral width of 6760 Hz. The following delays were used: $t_1^a(0) = 265$ μs, $t_1^c(0) = 4.865$ ms, $\tau = 4.6$ ms, $t_1^c(N) = 200$ μs. Time-domain convolution of the water frequency was performed (*14*). A squared sine bell, shifted 45°, was applied in t_1. The data were zero filled for digital resolutions of 6.6 and 3.3 Hz/point in the directly and indirectly detected dimensions, respectively. The ridge at 3.8 ppm is due to the protonated Tris.

If $\tau = (2J_{IS})^{-1}$ is assumed, at point C, scalar refocusing has occurred:

$$\{\cos\Omega_I(t_1^a + t_1^b - t_1^c)[I_y\cos\Omega_I\tau - I_x\sin\Omega_I\tau]$$

(multiple-quantum path)

$$-\sin\Omega_I(t_1^a + t_1^b - t_1^c)[I_x\cos\Omega_I\tau + I_y\sin\Omega_I\tau]\}\cos\Omega_S t_2$$

(single-quantum path). [3]

If relaxation during t_2 and multiplicity were identical for the multiple- and single-quantum pathways, the above expression would immediately simplify to

$$[I_y\cos\Omega_I(t_1^a + t_1^b - t_1^c + \tau) - I_x\sin\Omega(t_1^a + t_1^b - t_1^c + \tau)]\cos\Omega_S t_2. \quad [4]$$

As this is generally not the case, a second transient with orthogonal phases for ϕ_3, ϕ_4, and ϕ_5 (see the legend to Fig. 1) is needed to account for these differences (*6*). This phase shift results in the interchange of the single- and multiple-quantum pathways and the relevant terms at point B are

$$-[2I_zS_y\cos\Omega_I(t_1^a + t_1^b - t_1^c) + 2I_yS_y\sin\Omega_I(t_1^a + t_1^b - t_1^c)]\cos\Omega_S t_2. \quad [5]$$

The subsequent terms at point C originating from this coherence are the negation of the terms listed in expression [3]. By subtracting the two transients, the modulation in expression [4] is obtained. Thus, the chemical shift of spin I evolves throughout $t_1 = t_1^a + t_1^b - t_1^c + \tau$, independent of t_2.

The experiment is carried out with the following delays and increments. The initial values of the delays are $t_1^a(0)$ = duration of G_1 gradient delays plus the length of the π pulse on S; $t_1^b(0) = 0$; $t_1^c(0) \leq (2J_{IS})^{-1}$; and $\tau = t_1^c(0) - t_1^a(0) - 4\delta_{190°}/\pi$, where $\delta_{190°}$ is the width of the pulse on I with a $\pi/2$ flip angle. The total acquisition time in t_1 is

$$AT_1 = t_1^a(N) + t_1^b(N) - t_1^c(N) + \tau = (N-1)/SW_1,$$

where the spectral width in t_1, SW_1, equals $(\Delta t_1^a + \Delta t_1^b - \Delta t_1^c)^{-1}$, and N is the number of complex points acquired. With $t_1^a(N) = t_1^a(0) + (N-1)\Delta t_1^a$, one finds the increments

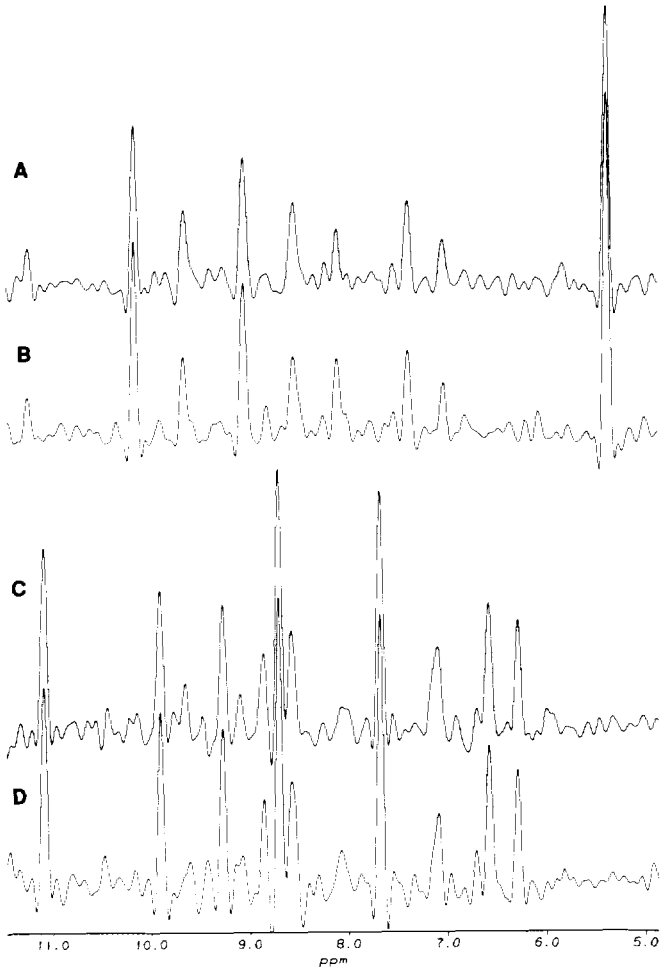

FIG. 3. Illustration of the line-narrowing effect in HSMQC-NOESY using full-sweep semiconstant time. B and D from the spectrum in Figure 2 are compared with A and C from a conventional HSMQC-NOESY (*15*) acquired with the same relevant parameters. A and B were taken at −0.69 ppm while C and D were taken at 6.20 ppm, from uncrowded regions of the spectrum as indicated in Fig. 2.

$$\Delta t_1^a = \{[(N-1)/SW_1] + (2J_{IS})^{-1} - \tau - 2t_1^a(0)\}/[2(N-1)],$$

$$\Delta t_1^b = \{[(N-1)/SW_1] - (2J_{IS})^{-1} + 2t_1^c(N) - \tau\}/[2(N-1)],$$

$$\Delta t_1^c = [t_1^c(N) - t_1^c(0)]/(N-1),$$

where $t_1^c(N)$ is the length of gradient G_1, typically ~ 100 μs for the gradient pulse and ~ 100 μs for gating it on and off.

Figure 2 illustrates that the FSCT-HSMQC-NOESY sequence described in Fig. 1 gives rise to clean spectra of 1.8 m*M Escherichia coli* flavodoxin at 500 MHz. Artifacts in this data potentially arise from the nonideality of the traveling ^{1}H π pulse. These artifacts can be suppressed by either employing the pulsed field gradients shown or by applying Exorcycle (*7*) to this π pulse. As of the Nth point in t_1, the duration of the pulse sequence is shorter by $1/J_{IS}$ than a conventional sequence without overlapping t_1 period. In practice, the gains are perhaps about $0.85/J_{IS}$ as defocusing and refocusing delays are optimized to minimize effects of relaxation. This gives rise to an apparent decrease in the rate of relaxation during t_1 of by a factor of about $(AT_1 - 0.85/J_{IS})/AT_1$. Another small advantage is that the homonuclear J_{II} coupling also evolves for $0.85/J_{IS}$ less time. Columns along F_1 show the narrowing in FSCT-HSMQC-NOESY (Figs. 3B and 3D) relative to the conventional spectrum (Figs. 3A and 3C). Relative line narrowing more dramatic than this can be obtained when shorter ^{1}H t_1 acquisition times, approaching $1/J_{IS}$, are used, e.g., in 4D isotope-edited NOESY experiments. As seen in Fig. 3, a sensitivity enhancement is realized by the FSCT-HSMQC-NOESY experiment over the conventional ^{15}N HSMQC-NOESY experiment.

The linewidth advantages can also be obtained using double semiconstant time (DSCT), proposed recently for HMQC-type experiments (*5*). However, the DSCT approach introduces three additional π pulses relative to the conventional experiment, which we have found to be particularly problematic. First of all, the imperfections of the additional π pulses reduce the sensitivity of DSCT-H(S)MQC-NOESY. Second, the additional pair of incremented π pulses in the DSCT approach introduces more artifacts to be suppressed by PFGs or more extensive phase cycling. Where pulsed field gradients are not available, the FSCT-HSMQC-NOESY can be implemented by using a 32-step phase cycle as indicated in the legend to Fig. 1. For the DSCT version without gradients, Exorcycle is needed on both traveling ^{1}H π pulses for an impracticable 128 steps.

The overlap methods FSCT-H(S)MQC and DSCT-H(S)MQC do not permit the use of field gradients in *zz* filters for solvent suppression, as is possible in HSQC. This limitation is irrelevant for 3D or 4D ^{13}C-edited NOESY and for 4D ^{13}C/^{15}N NOESY. When FSCT is implemented in ^{13}C editing, the one additional ^{1}H π pulse may cause some sensitivity loss, offsetting gains from the line narrowing. Very attractive applications of full-sweep HSMQC methods exist in out-and-back-style triple-resonance experiments, where a pair of π pulses is actually removed from the sequence, as discussed below.

The 4D HNCAHA experiment (*8, 9*) suffers from severely limited resolution in the constant-time $^{13}C^{\alpha}$ dimension. If the HSQC transfer between $^{13}C^{\alpha}$ and $^1H^{\alpha}$ were changed to an HMQC, the method of Madsen and Sørensen (*3*) could be applied to obtain twofold more resolution. However, Boucher *et al.* (*9*) showed that the HSQC version gives a clearly better lineshape in the $^1H^{\alpha}$ dimension (and

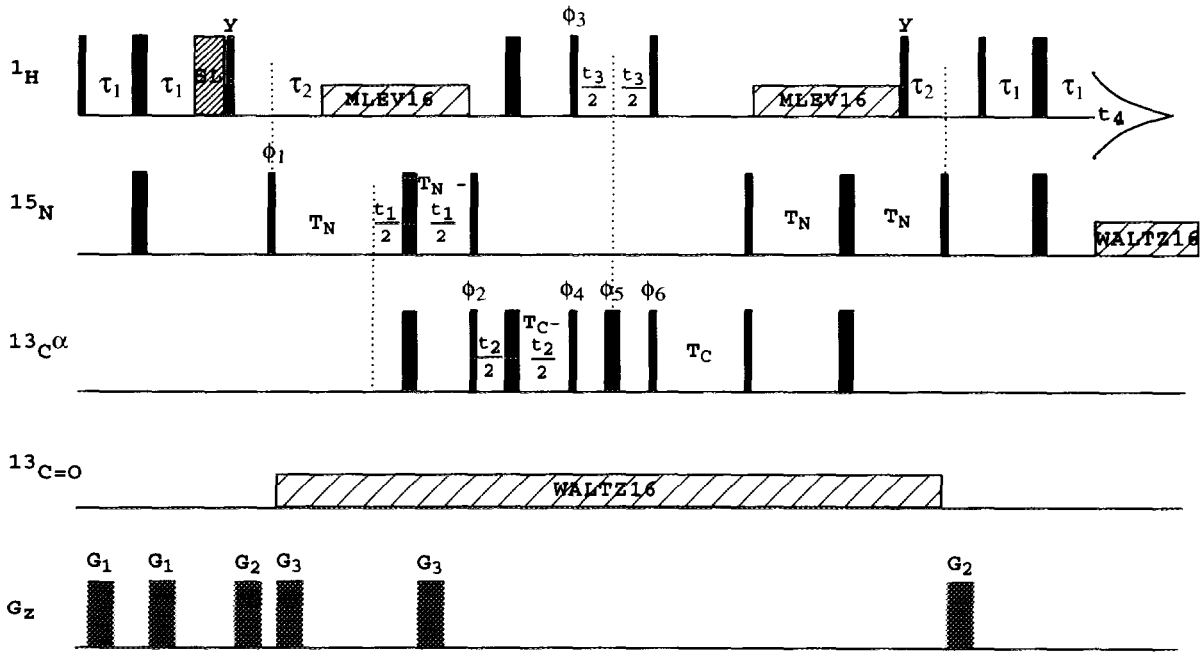

FIG. 4. Pulse sequence of the HNCAHA experiment with full-sweep constant-time measurement of $^{13}C^\alpha$ chemical shift during an HSMQC transfer between $^{13}C^\alpha$ and $^1H^\alpha$. Narrow and wide pulses represent $\pi/2$ and π flip angles, respectively. The first and last ^{15}N π pulses were composite. Unlabeled pulses are applied along the x axis. The phase cycling is $\phi_1 = x, x, -x, -x$; $\phi_2 = x$; $\phi_3 = x, -x$; $\phi_4 = 4(x), 4(y)$; $\phi_5 = 4(x), 4(y)$; $\phi_6 = 4(-x), 4(-y)$; and receiver = $x, -x, -x, x, -x, x, x, -x$. States–TPPI quadrature (*13*) is applied to ϕ_1, ϕ_2, and ϕ_3. Delays were $\tau_1 = 2.3$ ms; $\tau_2 = 5.4$ ms; $T_N = 12$ ms; $T_C = 3.2$ ms. The spin-lock pulse (*16*) was 1 ms long. The durations and strengths of the gradients along the z axis were $G_1 = 1.25$ ms, 10 G/cm; $G_2 = 2$ ms, 12 G/cm; $G_3 = 1.35$ ms, 13 G/cm. A radiofrequency field strength of about 300 Hz was used to decouple the $^{13}C{=}O$ spectrum with WALTZ-16 (*17*). No water presaturation was applied.

thus better sensitivity) than the HMQC version due to the effect of the passive $J_{C\alpha\beta}$ coupling on the latter. Employing the HSMQC transfer instead, much of the linewidth and sensitivity advantage of the HSQC version can be recovered. Using the method of full-sweep, constant time (FCT) in HSMQC described above, we can achieve a dramatic twofold resolution enhancement in the $^{13}C^\alpha$ dimension (Fig. 5) while keeping the total delay time in the pulse sequence the same (Fig. 4). The phase cycle must be shortened from the published 16-step cycle in order to take advantage of the twofold resolution gain in the $^{13}C^\alpha$ dimension. Use of the spin-lock pulse, first pair of gradient pulses, and first zz filter with gradient allows removal of the inversion of the first (or second) ^1H $\pi/2$ pulse ordinarily used for suppression of axial magnetization (*10*). Using the resulting eight-step phase cycle with the pulsed field gradients shown in Fig. 4, artifact and water suppression are excellent. The resolution gain in the ^{13}C dimension from acquiring twofold more points is clear in Fig. 5. However, one anticipates line-broadening effects in the $^1H^\alpha$ dimension because of an admixture of $^{13}C^\alpha$, $^1H^\alpha$ multiple-quantum coherence into the $^1H^\alpha$ single-quantum coherence. Fortunately, the effect upon $^1H^\alpha$ lineshape is minor as documented by a comparison of vectors from the HSQC (Fig. 6A) and revised HSMQC (Fig. 6B) versions of the HNCAHA. The FCT-HSMQC modification of the HNCAHA experiment makes possible good resolution in the $^{13}C^\alpha$ dimension without sacrificing resolution in the other dimensions. The use of "mirror-image" linear extension (*11*) in the ^{15}N and ^{13}C dimensions should make the resolution in this 4D experiment quite adequate for assignment purposes.

In summary, applications for overlapping chemical-shift evolution periods with both the defocusing and refocusing scalar-evolution periods of H(S)MQC editing steps have been extended. The method of doubling resolution in constant-time periods (*3*) can be applied not only to HMQC-style but also to HSMQC-style labeling of heteronuclei, permitting a lineshape advantage in some experiments. The technique has been adapted to semiconstant-time periods, bringing about ^1H line narrowing in experiments such as HSMQC-NOESY. Compared with the approach of sweeping two pairs of π pulses (*4, 5*), the full sweep of a single pair of π pulses generates fewer artifacts to be suppressed by gradients or Exorcycle phase cycling.

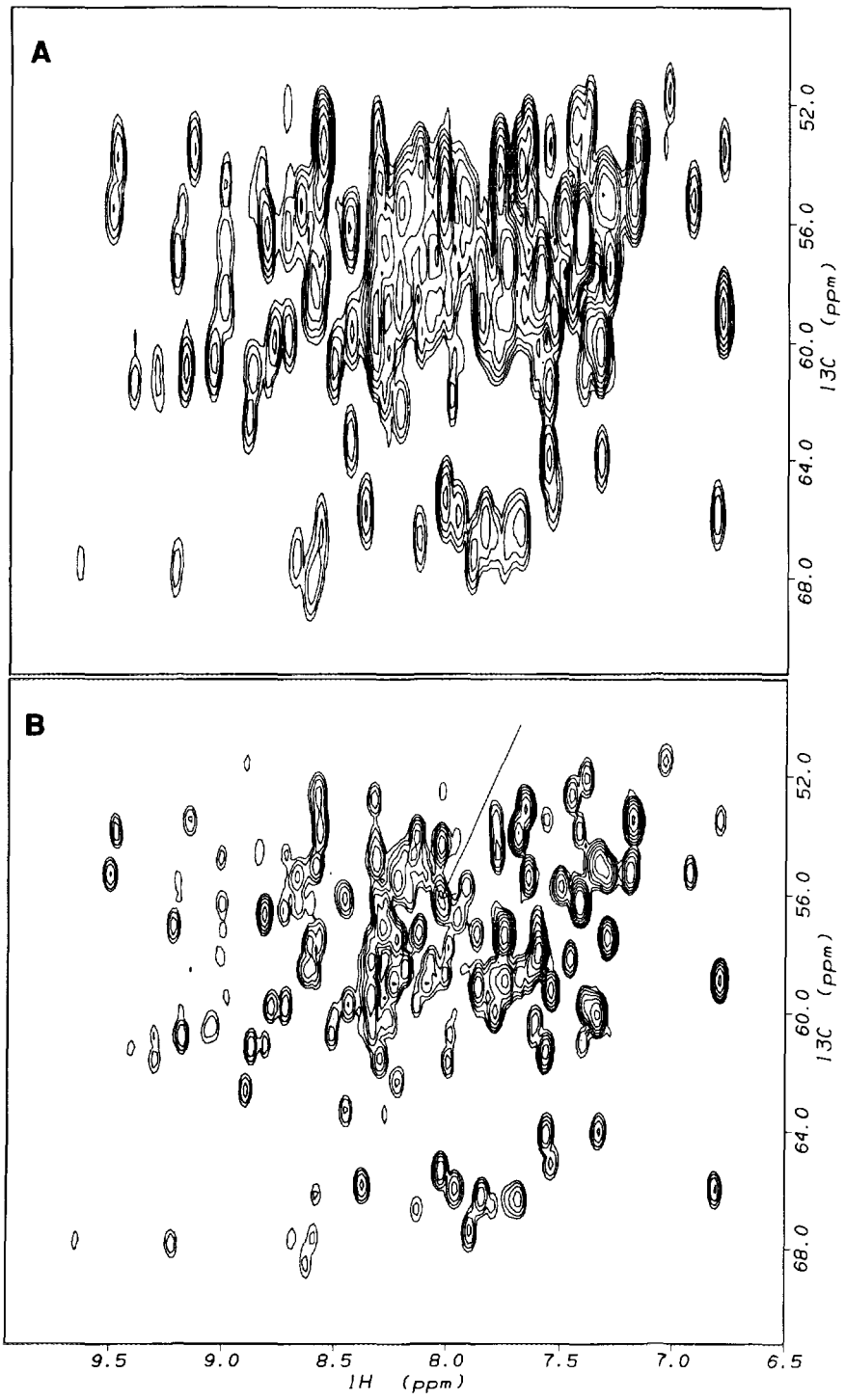

FIG. 5. Comparison of the $^{13}C^{\alpha}$ resolution obtainable from (A) the HNCAHA experiment previously described (*8*), which uses a conventional constant-time period with an HSQC transfer between $^{13}C^{\alpha}$ and $^{1}H^{\alpha}$, and from (B) the FCT-HNCAHA experiment described in the legend to Fig. 4, which utilizes full-sweep constant-time shift labeling during the HSMQC transfer between $^{13}C^{\alpha}$ and $^{1}H^{\alpha}$. The parameters of the pulse sequence used to collect spectrum A were the same as those listed in the legend to Fig. 4 but $\phi_2 = 4(x), 4(-x)$; $\phi_4 = y$; $\phi_5 = x$; $\phi_6 = y$, and an additional pair of π pulses at $^{13}C^{\alpha}$ and $^{1}H^{\alpha}$ frequencies were of course applied during the refocusing period of the HSQC transfer. The spectra were acquired on a Bruker AMX-500 equipped with a fourth channel described previously (*18*), pulsed field gradients, and a triple-resonance probe. A and B are skyline projections of 3D spectra of 1 m*M* T4 lysozyme, 30°C, in which $^{1}H^{N}$, $^{13}C^{\alpha}$, and $^{1}H^{\alpha}$ frequencies were measured. Using a $^{13}C^{\alpha}$ spectral width of 3760 Hz, 12 complex points were collected for spectrum A and 24 complex points were collected for spectrum B. In the $^{13}C^{\alpha}$ dimension, a 60°-shifted squared sine bell was applied and zero filling used for a digital resolution of 29.4 Hz per point. No linear prediction was used. Over a $^{1}H^{\alpha}$ spectral width of 1890 Hz, 32 complex points were collected and a Kaiser window was applied. Total acquisition time was 23.5 hours each using 48 scans per FID for A and 24 scans per FID for B.

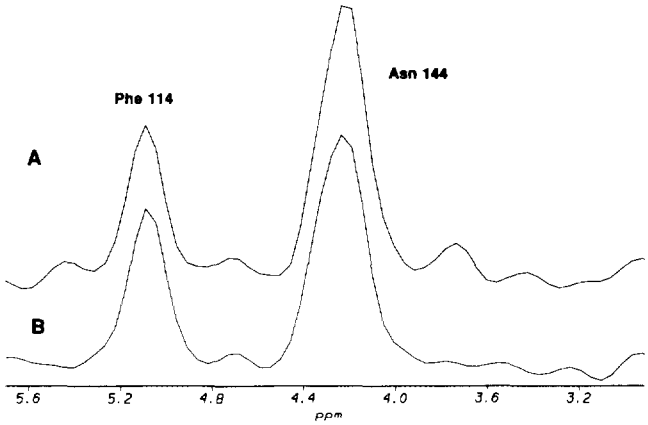

FIG. 6. Comparison of the $^1H^\alpha$ lineshape in the spectra in Figs. 5A and 5B. A vector along the $^1H^\alpha$ dimension through the peak indicated in Fig. 5B was taken through the intraresidue peaks of Phe 114 and Asn 114 of the HSQC-type spectrum (A) and of the revised FCT-HSMQC-type spectrum (B).

ACKNOWLEDGMENTS

We thank Dr. Martha Ludwig for the gift of *E. coli* flavodoxin and Dr. Frederick Dahlquist for the gift of T4 lysozyme. We thank Mark Fischer and Dr. Ananya Majumdar for communicating T4 lysozyme assignments. Generous contributions of computer equipment by Parke-Davis/Warner Lambers are acknowledged. This work is supported in part by American Cancer Society Grant PF-4056 to S.R.V. and by NSF Grant MCB-9218573 to E.R.P.Z.

REFERENCES

1. S. Grzesiek and A. Bax, *J. Biomol. NMR* **3,** 185 (1993).
2. T. M. Logan, E. T. Olejniczak, R. X. Xu, and S. W. Fesik, *J. Biomol. NMR* **3,** 225 (1993).
3. J. C. Madsen and O. W. Sørensen, *J. Magn. Reson.* **100,** 431 (1992).
4. G. W. Vuister and A. Bax, *J. Am. Chem. Soc.* **115,** 7772 (1993).
5. D. R. Muhandiram, G. Y. Xu, and L. E. Kay, *J. Biomol. NMR* **3,** 463 (1993).
6. E. R. P. Zuiderweg, *J. Magn. Reson.* **86,** 346 (1990).
7. R. Freeman and J. Keeler, *J. Magn. Reson.* **43,** 483 (1982).
8. E. T. Olejniczak, R. X. Xu, A. M. Petros, and S. W. Fesik, *J. Magn. Reson.* **100,** 444 (1992).
9. W. Boucher, E. D. Laue, S. L. Campbell-Burk, and P. J. Domaille, *J. Biomol. NMR* **2,** 631 (1992).
10. A. Bax and S. Pochapsky, *J. Magn. Reson.* **99,** 638 (1992).
11. G. Zhu and A. Bax, *J. Magn. Reson.* **90,** 405 (1990).
12. D. J. States, R. A. Haberkorn, and D. J. Ruben, *J. Magn. Reson.* **48,** 286 (1982).
13. D. Marion, M. Ikura, R. Tschudin, and A. Bax, *J. Magn. Reson.* **85,** 393 (1989).
14. D. Marion, M. Ikura, and A. Bax, *J. Magn. Reson.* **84,** 425 (1989).
15. E. R. P. Zuiderweg, L. P. McIntosh, F. W. Dahlquist, and S. W. Fesik, *J. Magn. Reson.* **86,** 210 (1990).
16. B. A. Messerle, G. Wider, G. Otting, C. Weber, and K. Wüthrich, *J. Magn. Reson.* **85,** 608 (1989).
17. A. J. Shaka, J. Keeler, T. Frenkiel, and R. Freeman, *J. Magn. Reson.* **52,** 335 (1983).
18. S. R. Van Doren and E. R. P. Zuiderweg, *J. Magn. Reson.* **104,** 222 (1993).